Boletín Geológico

SERVICIO GEOLÓGICO COLOMBIANO

Boletín Geológico, 47, 67-84, 2020
https://doi.org/10.32685/0120-1425/boletingeo.47.2020.492

Received: May 14, 2020
Revised: June 2, 2020
Accepted: September 28, 2020
Published online: December 28, 2020

Listvenites: new insights of a hydrothermal system fossilized in Cerro Matoso peridotites, Montelíbano, Córdoba Department, Colombia

Listvenitas: nuevos vestigios de un sistema hidrotermal fosilizado en las peridotitas de Cerro Matoso, Montelíbano, departamento de Córdoba, Colombia

Andrés **Castrillón**[1], Javier **Guerrero**[1]

1 Departamento de Geociencias, Universidad Nacional de Colombia, Bogotá, Colombia
Corresponding author: Andrés Castrillón, acastrillon@unal.edu.co

Abstract

The products of metasomatic alteration (e.g., carbonation) of peridotites are called listvenites. Based on a description of the outcrops in the laterite deposit at Cerro Matoso located in the NW of Colombia, the mineralogical composition confirmed by petrography, and a chemical analysis performed with XRF and WDS/EDS, the previous unit called tachylite is redefined as listvenite. Two types of listvenites are described: listvenite A, with the mineralogical association of quartz + siderite + phyllosilicates + goethite +/- magnetite, and listvenite B, with the association of siderite + phyllosilicates + goethite. Cr-spinel relics accompanied by Mn-siderite and neoblastic textures, indicate their origin from peridotites, where Mn-Fe would have been deposited by hydrothermal fluids. Hydrothermal reducing environments with alkaline fluids and low temperatures should have favored the formation of listvenites that are observed along a fracture zone, oriented WNW-ESE at Pit-1 in Cerro Matoso. Due to exposure to climatic conditions since the Eocene, but definitively since the last Andean Orogeny, listvenites were affected, like all the rocks in the Cerro Matoso deposit, by intense supergene weathering and leaching processes, which could make their true origin unclear.

Keywords: Listvenite, metasomatism, hydrothermal systems, Cerro Matoso, spinel.

Resumen

El producto de alteración metasomatica (e.g., carbonation) de peridotitas son listvenitas. Basados en una descripción de los afloramientos en el depósito de lateritas niquelíferas de Cerro Matoso, localizado al NW de Colombia, la composición mineralógica confirmada con XRD y análisis químicos con XRF y WDS/EDS, se redefine una unidad previamente llamada tachyilita como listvenita. Se describen dos tipos de listvenitas; listvenita A con la asociación mineralógica: cuarzo + siderita + filosilicatos + goetita

Citation: Castrillón, A., & Guerrero, J. (2020). Listvenites: new insights of a hydrothermal system fossilized in Cerro Matoso peridotites, Montelibano, Córdoba Department, Colombia. *Boletín Geológico*, 47, 67-84, https://doi.org/10.32685/0120-1425/boletingeo.47.2020.492

+/- magnetita, y listvenita B con la asociación: siderita + filosilicatos + goetita. Relictos de Cr-espinela, acompañados por Mn-siderita y texturas neoblásticas, indican un origen a partir de peridotitas, en donde Mn-Fe serían aportados por fluidos hidrotermales. Ambientes hidrotermales reductores con fluidos alcalinos y de bajas temperaturas debieron favorecer la formación de listvenitas, que se observan a lo largo de una zona de fracturas orientada WNW-ESE en el Pit-1 de Cerro Matoso. Expuestas a condiciones climáticas quizás desde el Eoceno pero definitivamente desde la última Orogenia Andina, las listvenitas fueron afectadas al igual que todas las rocas en el depósito de Cerro Matoso por intensos procesos de meteorización y lixiviación mineral ocultando el verdadero origen de algunas.

Palabras clave: Listvenita, metasomatismo, sistemas hidrotermales, Cerro Matoso, espinelas.

1. Introduction

Listvenite (from the Russian "listvenity", Rose, 1837) is a term used principally by Russian geologists to describe the carbonate +/- sericite +/- pyrite alteration of mafic and ultramafic ophiolitic assemblages, which indicates the hydrothermal involvement of quartz +/- carbonate veins (Rose, 1837). This alteration is due to carbonation occurring in rocks that are susceptible to interactions with CO_2-rich fluids, resulting in the alteration and precipitation of carbonate and other minerals (Halls and Zhao, 1995). Some authors recommend that the term listvenite be used strictly in cases where potassium metasomatism has been verified in ultramafic rocks (serpentinites, serpentinized peridotites) and where this potassium metasomatism is evidenced by the development of micas (e.g., fuchsite) as components of the mineralogical association included in "listwaenite" (Halls and Zhao, 1995; Abuamarah, 2020). Mafic and ultramafic rocks are particularly prone to carbonation due to abundant olivine $(Mg, Fe)_2SiO_4$ and pyroxene $(Ca, Mg, Fe)_2Si_2O_6$, which react with H_2O and CO_2 to form hydrous silicates, such as serpentine, Fe-oxides (magnetite) and carbonates (Kelemen and Matter, 2008). According to Halls and Zhao (1995), the correct spelling of the word listwaenite is listvenite, and it was proposed to describe the formations in Beresovsk in the Ural Mountains of central Russia (Halls and Zhao, 1995) and in Europe and North America (Bates and Jackson, 1987).

The term listvenite has been used for the following mineral assemblages: a quartz + magnesite rock derived from serpentinite at low temperatures by full conversion of all original Mg-silicates to carbonate and residual quartz (Bucher and Stober, 2019); quartz (45-55%) and carbonates (40-60%) with minor amounts of serpentine, chlorite, chromite, and Cr-rich sericite (fuchsite) (e.g., upper mantle peridotites in the Cryogenian Bir Umq ophiolite, Arabian Shield, Saudi Arabia, Abuamarah, 2020); and listvenites (silica-type) mainly consisting of opal, quartz, cristobalite, chalcedony, and relicts of serpentine, Cr-spinel and secondary iron hydroxides, where magnesite, dolomite, calcite and clay minerals are minor phases (e.g., Khoy ophiolite complex, northwestern Iran, Imamalipour et al., 2018). The term listvenite has also been used to describe the mineral association of metamorphosed amphibole-bearing listvenites (e.g., Bayazeh Paleozoic ophiolite, Nosouhian et al., 2016, 2019). In this text, the term listvenite refers to a variation of carbonated and silicified serpentinite to denote rocks that are strictly the metasomatic product of low-grade hydrothermal alteration of ultramafic rocks and can be defined as one rock type or a mixture of rock types that are genetically related to the same hydrothermal event but can vary depending on the intensity of the alteration and the composition of the protoliths (e.g., Kashkai and Allakhverdiev, 1965; Buisson and Leblanc, 1987; Leblanc, 1991; Halls and Zhao, 1995).

According to Ucurum (2000), the movement of hydrothermal fluids along fractures of ultramafic rocks produces dikes of listvenites whose length can vary by hundreds of meters, and whose thickness can vary by tens of meters. These rocks have been found in altered mafic and ultramafic rocks in British Columbia (Ash and Arksey, 1990), Turkey (Ucurum, 1998, 2000), Canada (Jutras and Geol, 2002), Mali, Morocco and Saudi Arabia (Buisson and Leblanc, 1987; Leblanc, 1991) and are now identified in the deposit of Cerro Matoso, NW Colombia. Listvenites in Cerro Matoso are covered by marine deposits of black conglomeratic mudstone and are located along a fracture zone oriented WNW-ESE.

The Cerro Matoso ultramafic rocks, developed a Ni laterite profile by weathering with different characteristics in the south (or Pit-2) (Figure 1), with nickel grades not exceeding 4%, compared with the laterite profile developed in the north (or Pit-1), where nickel grades reached 9%. The higher nickel grades at Pit-1

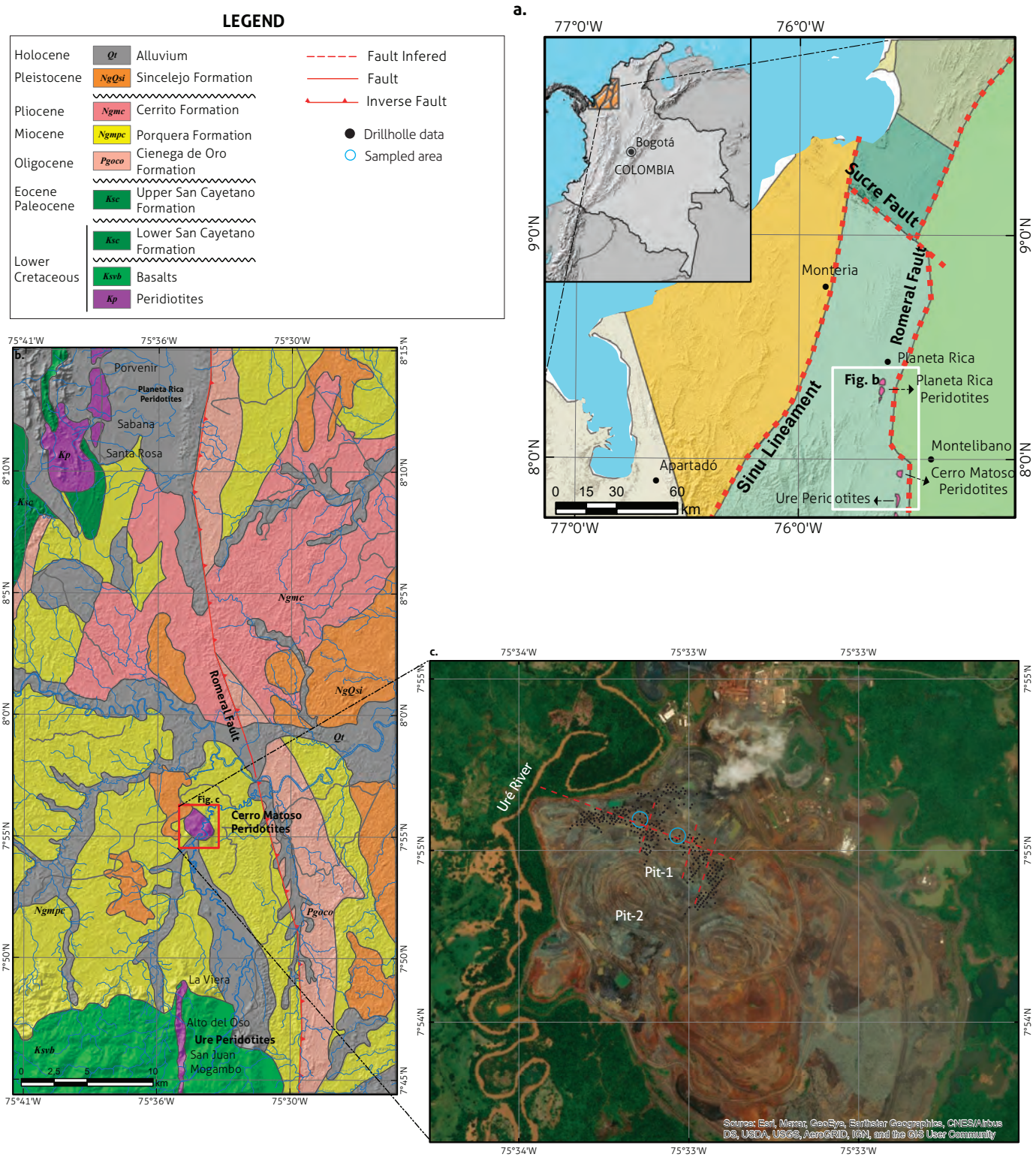

Figure 1. Regional geology and location of the Cerro Matoso Ni laterite deposit and of Pit-1 and Pit-2
Location of listvenites along Pit-1 in the Cerro Matoso open pit mine, illustrating the WNW-ESE general trend (modified from Londoño and González, 1997; Gleeson et al., 2004). The peridotites of Cerro Matoso are surrounded by basalts (Ksvb) (outcropped 30 km to the south), which are unconformably covered by early- and mid-Miocene sediments from the Ciénaga de Oro Formation (Pgoco), Porquera Formation (Ngmpc), Cerrito Formation (Ngmc) and Sincelejo Formation (NgQsi).

are related to the influence of hydrothermal systems, and the "tachylite" (a term used by mine geologists to describe an enigmatic Fe-oxide horizon) was assigned to the laterite profile, although it was not considered to be a normal product of peridotite weathering (Gleeson et al., 2004). A detailed petrological and geochemical study of "tachylite" occurrence was published by Sumicol (2002). This paper describes the characteristics, mineralogy, and geochemistry of an association of rocks in the Cerro Matoso nickel laterite deposit that could correspond to listvenites.

2. Regional geological setting

The Cerro Matoso deposit is located in the department of Córdoba, northwest Colombia. Nickeliferous laterites are the product of supergene weathering of peridotites (principally harzburgites with varying degrees of serpentinization). Peridotites of Cerro Matoso are defined as an isolated body of outcrops that have been assigned to an Early Cretaceous ophiolite complex (Mejia and Durango, 1981). The ultramafic rocks are associated with the ancient oceanic crust that existed in the Pacific Ocean, west of its present position (Pindell and Barrett, 1990; Pindell and Kennan, 2009), where it is suggested that the mantle rocks were exhumed as an Oceanic Core Complex (OCC) (Castrillón, 2013). The OCC is part of the ophiolites accreted during the pre-Andean orogeny along the Romeral Fault System, which is considered an important boundary between the oceanic crust to the west and the continental crust to the east (Barrero, 1974; Meissener et al., 1976). As the American continent moved west and the oceanic plate moved east during the Late Cretaceous, ocean segments accreted in the western part of the continent (Lewis et al., 2006) were eventually exposed to supergene weathering conditions beginning in the late Eocene (López-Rendón, 1986). Locally, the CM peridotites are overlaid by a deep marine sedimentary succession (Castrillón, 2013). These sediments were interpreted to be part of the ultramafic weathering profile (López-Rendón, 1986; Gonçalves et al., 1999; Gleeson et al., 2004, Lelis et al., 2004). Recently, Castrillón (2019) suggested that fossils and black conglomeratic mudstone found at Pit-1 represent ocean floor sediments associated with hydrothermal systems hosted by ultramafic rocks.

The variably serpentinized ultramafic rocks of Cerro Matoso that developed a complete laterite profile, where iron and nickel alloy is produced in the mining process, are exposed in the form of an elongated isolated hill approximately 2.5 km long and 1.5 km wide at the northern limit of the Western Cordillera and are considered the northernmost extension of the allochthonous oceanic crustal terranes (Mora-Bohórquez et al., 2017). The peridotites of Cerro Matoso are surrounded by basalts (Ksvb) (outcropped 30 km to the south), which are unconformably covered by sediments from the early and mid-Miocene, including a transgressive succession consisting of fluvial and shore sandstones of the Ciénaga de Oro Formation (Pgoco), followed by marine shales of the Porquera Formation (Ngmpc), which are unconformably covered by Cerrito Formation (Ngmc) and Sincelejo Formation (NgQsi) sediments. The Cerro Matoso peridotites have been exposed on the surface since the middle Eocene and have therefore been affected by intense weathering (e.g., López-Rendón, 1986; Gleeson et al., 2004). According to López-Rendón (1986), lateritization probably started in the late Eocene-early Oligocene, and chemical weathering and erosion continued throughout the Oligocene (Figure 1).

3. Sample and method

According to the field description, listvenites are very fine-grained and extremely friable; they have conchoidal fractures and high porosity, a violet-brown to black color when dry, and a dark-green color when wet, and have locally abundant quartz veins (Figure 2a). Listvenites underlie the black conglomeratic mudstone (Figure 2b) and are a very uniform unit, consisting of lenses capping altered peridotites (i.e., green saprolites). Two listvenite varieties can be differentiated according to their veinlets and brecciated texture (Figure 2a-2c). A representative set of samples (Figure 3a-3f) was collected at the 49 Bench level of Pit-1, where two varieties coexist (A: CM-3, CM-4, CM-6, CM-7; and B: CM-27, CM-56, samples) overlaying green saprolites along transitional contacts (Figure 3g-3h), altered peridotites (Figure 3i), peridotites with magnesite veins (Figure 3j) and peridotites (Figure 3k-l). Petrographic classification and analysis were performed using a Carl ZEISS Primo Star HD/cam Full Köhler microscope, 100x, SF2, from the Instituto de Geología of the Universidad Nacional Autónoma de México (UNAM). Scanning electron microscopy (SEM) and X-ray diffraction (XRD) patterns were further used for the identification of minerals in listvenites. According to their textures and silica content, three samples of listvenite were selected for further analysis: sample CM-6 (brecciated texture) and samples CM-27 and CM-56, also named DRX14 (non-brecciated texture); these were analyzed at the UNAM labs, and sample CM-3 was selected for XRF and analyzed at the Gmas labs (code name CM-14).

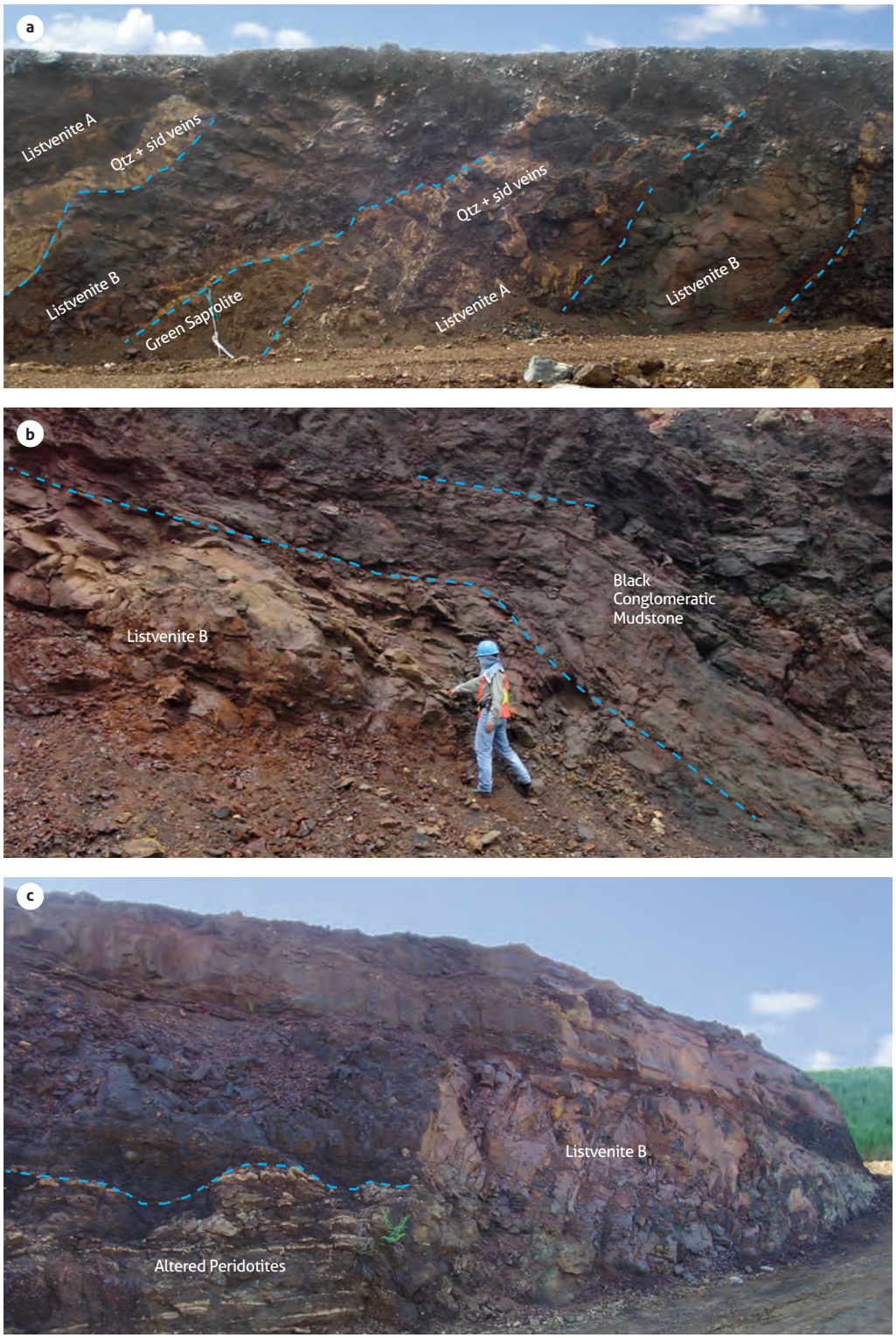

Figure 2. Listvenites outcrops at Pit-1 of Cerro Matoso
a) Western orientation of the main fractures presented by the listvenites (varieties A and B). Variety A presents a complex vein pattern on top of the green saprolite. Variety B, with a dark purple color, has lenses with or without silica/siderite veins. b) Black conglomeratic mudstone (BCM) overlying listvenites. c) Altered peridotites underlying a listvenite cap (Bench level 49 of Pit-1; outcrop is 8 m high). A purple color is also observed with bronze tones, typical of listvenites when dry (Bench level 56 of Pit-1; outcrop is 7 m high).

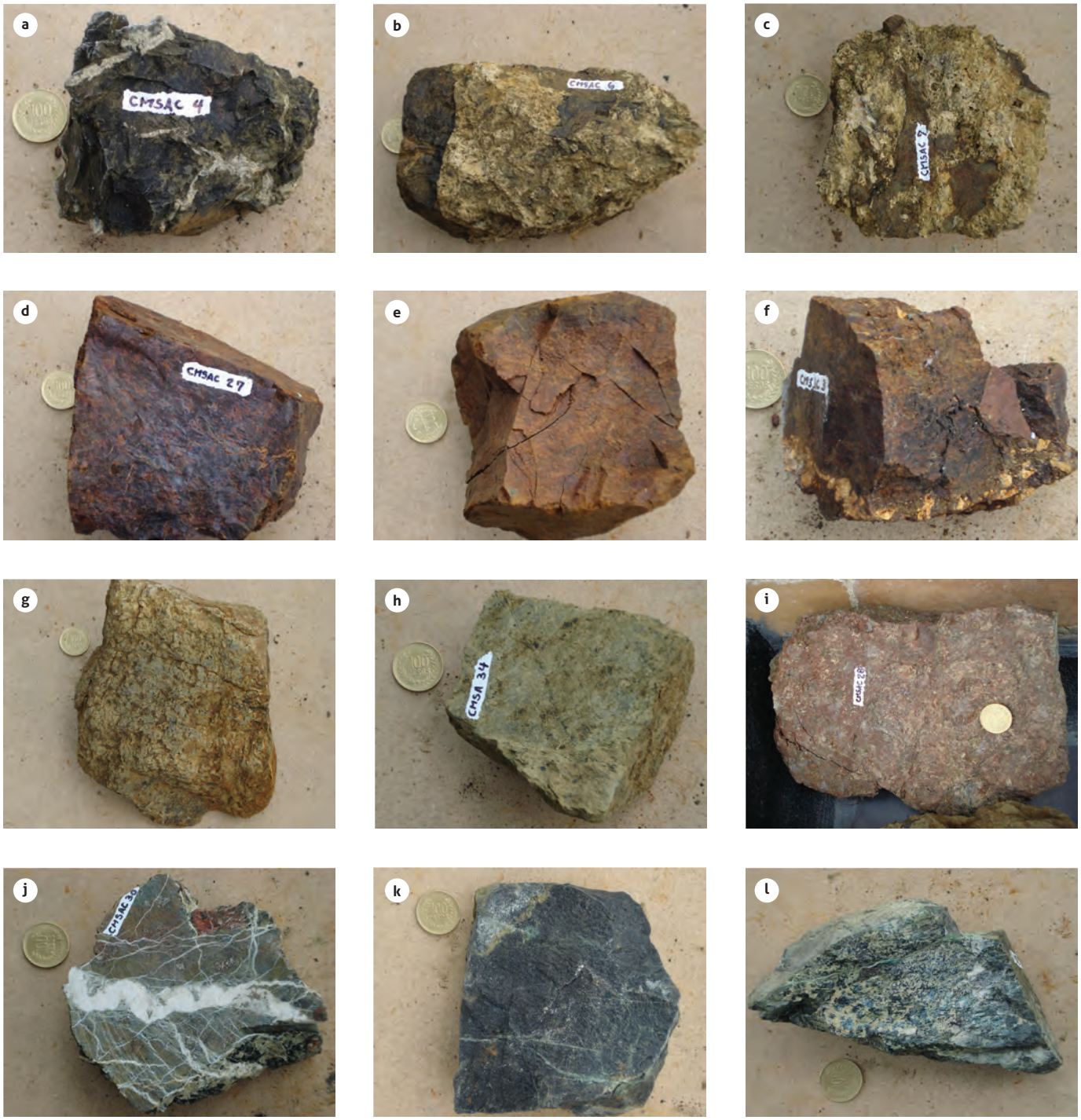

Figure 3. Hand samples collected from the Cerro Matoso deposit at Pit-1
a-c, f) Listvenite variety A is characterized by brecciated textures with high silica/siderite vein content. In some cases, listvenite was fractured into angular clasts several mm to 20 cm in size and cemented by quartz veins. d-e) Listvenite variety B is characterized by a purple color. g) Low-Mg green saprolite. h) High-Mg green saprolite. i) Saprolitized peridotite. j) Magnesite and silica veins in peridotite. k) Fresh peridotite. l) Serpentinized peridotite.

Selected samples for bulk-rock mineralogical analysis were ground with an agate mortar and pestle to >200 µm and mounted in aluminum holders for X-ray powder diffraction analysis following the standard XRD procedures (Brindley and Brown, 1980; Moore and Reynolds, 1997). Measurements were made using an EMPYREAN diffractometer at the Instituto de Geología LANGEM, Universidad Nacional Autónoma de México and Gmas labs in Bogotá. The equipment was operated with an accelerating voltage of 45 kV and a probe current of 40 mA using CoKα radiation (cobalt tube) without a monochromator and iron filter in the incident optics of the equipment. The detector used is of solid state (PIXCel 3D). The preparations were measured over a 2θ angle range of 5-80° (air-dried) and 5-40° (glycolated and heated) in steps of 0.003° and 40 second integration time. Peak positions were standardized against the quartz 100 peak of relative intensity taken at 4.26 Å. The databases used for identification were the Inorganic Crystal Structure database (ICCD, V2016) and the International Center for Diffraction Data (ICDD). Phase identification and quantification by the Rietveld refinement method were performed with a PDF-2 database using HighScore 7 V4.5 software. Relevant data from the diffractometer used in the refinement are shown in Table 1. The refined specimen-dependent parameters included zero error, displacement error, polynomial fitting for the background with six coefficients, cell parameters, crystallite size, atomic coordinates, and isotropic temperature factors. The GOF (goodness of fit) values show the fit between the Rietveld refinement and the experimental profile.

Table 1. Data from the diffractometer used in the refinement

Geometry	Bragg-Brentano
Goniometer Radius	220 mm
Radiation Source	CoKα
Generator	45 kV, 40 mA
Tube	Fine Focus
Divergence Slit	1⁄2° (fixed)
Soller Slits	0.04° (incident and diffracted beam)
Incident Beam Optics	Parallel Mirror
Filter	Iron Filter
Detector	Solid State (PIXcel 3D)
Step Size	0.002°
Integration Time	40 s

The composition of major elements was obtained by X-ray fluorescence (XRF) in fused $LiBO_2/Li_2B_4O_7$ disks using a Bruker_S4_Explorer X-ray fluorescence spectrometer with a Rh-anode X-ray tube as a radiation source in the Gmas labs in Bogotá. Semiquantitative and quantitative analyses were performed using the QUANT-EXPRESS method (fundamental parameters; He, 1991) based on the certified USGS standard samples AGV1, BCR2, DST2, QLO1, G2 and W2A, with which the equipment is calibrated. Chemical composition of carbonates and oxides in the listvenite carbon-coated thin section were analyzed under energy dispersive spectroscopy (EDS), wavelength dispersion spectrometry (WDS) and X-ray spectroscopy (XRD) with an electronic probe microanalyzer (EPMA) JEOL JXA-8900XR and an SEM model JSM-6300 (both from the Instituto de Geología - UNAM) operated at 15 kV accelerating voltage. Measurements were performed on different minerals of the sample, and the compositions were obtained from different points on each mineral (i.e., siderite: 12 points, magnetite: 7 points, spinel: 6 points, and orthopyroxene: 6 points) to determine their usual chemical composition. The textural classification of the quartz considered the quartz type and the individual grain size as well as its crystal shapes and textures and the way the quartz related to the surrounding rock (Demoustier, 1995; Demoustier and Castroviejo, 1997; Demoustier et al., 1998).

4. Results

4.1 Listvenite mineralogy and petrography

Listvenite A corresponds principally to the matrix-supported brecciated textures with quartz + siderite + serpentine + goethite assemblages; zonate microcrystalline coarse quartz (Qvxg) (<10 mm) crystallized into posthumous cavities in symmetric and radiated plumose textures. Microcrystalline fine quartz (Qvxf) (0.1-1 mm) is usually crystallized in the inner parts of plumose textures. Siderite (Sid) is present in zonate textures and works as cement with quartz. Serpentine (Ser) and goethite (Go) are products of peridotite alteration. A massive replacement quartz (QeM) in the housing rock forms heterogeneous angular and subangular fragments in breccia samples CM3 and CM7 (Figure 4a-4e). Listvenites of type A are characterized by their siderite + quartz vein systems in the field.

Listvenite B consists mainly of smectite with goethite and siderite and relic spinel. The smectite is nontronite. Siderite occurs as subhedral crystals with high birefringence. Goethite occurs as opaque earthy black aggregates, usually in fissures and with magnetite. Relic subangular olivines with blueish to purple colors are scarce. The light green yellowish fibrous crystals are phyllosilicates (Figure 4f).

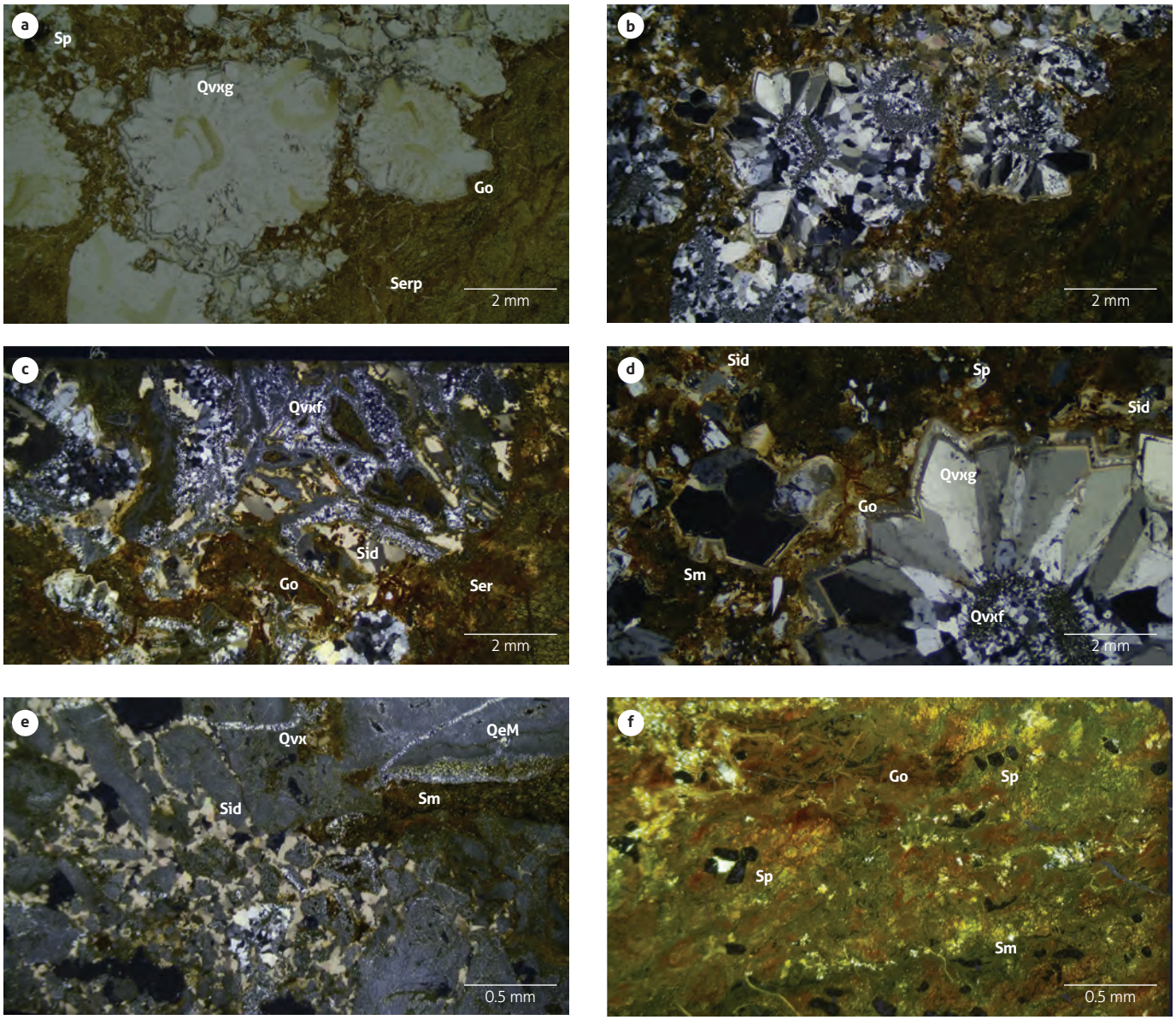

Figure 4. Listvenite thin sections
a and b) Listvenite A. Association of quartz + siderite + green serpentine (Ser) + quartz (Q)+ reddish goethite (Go). Posthumous cavities filled with thick microcrystalline quartz (Qvxg) in a symmetric feathery structure and radially zoned on the edges with fine microcrystalline quartz inside (Qvxf). Samples CM3_np_10x and nc. c) Listvenite A. Fine microcrystalline quartz (Qvxf) and siderite (Sid) as cement surrounded by goethite and serpentine (Ser). Sample CM3_nc_10x. d) Listvenite A. Detail of the feathery texture and zoned texture with siderite (Sid) on the edge of thick microcrystalline quartz (Qvxg). Fine microcrystalline quartz (Qvxf) with puzzled texture surrounded by smectite (Sm) and goethite (Go). Sample CM3_nc_20x. e) Brecciated matrix-supported texture with quartz and massive replacement of the host rock (QeM) forming fragments of heterogeneous subhedral to anhedral quartz with impure edges, siderite (Sid) as cement and micro veins of quartz (Q). Sample CM3_nc_40x. f) Listvenite B. Association of serpentine (Ser) + goethite (Go) +/- siderite (Sid), with euhedral spinels (Sp) as accessories. Sample CM27_nc_10x.

4.2 XRD Diffractometry

XRD for fractions >200 µm indicate siderite and phyllosilicates as the common minerals. In sample CM-56, siderite (5.7%), goethite (3.6%) and phyllosilicates 15 Å pbb-type smectite (90.7%) are the principal components. A more suitable smectite with a 15 Å peak was identified by the Green-Kelly test as nontronite (Sumicol, 2002). Sample CM-3 consists of quartz, siderite, goethite and phyllosilicates (serpentine). Sample CM-6 is composed of quartz, siderite, goethite, magnetite and phyllosilicates (serpentine) (Figure 5).

4.3 Electron microscopy

Sample CM-56 was analyzed under a scanning electron microscope. Cr-spinel relicts are very fractured and surrounded by Mn-siderite + smectite (Figure 6a and b). In Figure 6c, siderite occurs as subhedral to anhedral crystals in a neoblastic texture. Magnetite is tabular and appears in smaller amounts, typically < 5 vol. Orthopyroxene relics with border alteration of serpentine are commonly rimmed by magnetite (Figure 6d). In general, the dominant phase is smectite, which replaces serpentine. Olivine relics are also present in minor amounts as anhedral crystals.

4.4 Geochemistry

4.4.1 Major oxides

Geochemical analyses of sample CM-56 are shown in Table 2. For comparison, four representative analyses of listvenites, named "tachylites," from the Cerro Matoso open pit mine are also provided; all samples were collected from Pit-1. Listvenites contain silica between 27.5 and 65.3 wt% and Fe between 21.5 and 61.8 wt%, which are their principal components. Al_2O_3 (2.7 to 6.5 wt%) and Mg (<3.7 wt%) are low, resulting in lower MgO/SiO_2 ratios (0.02–0.46 wt%). The Ni content is between 1.6. and 6.1 wt%.

4.4.2 Microprobe chemical composition of siderite

The chemical composition (wds/eds) of siderite in the listvenite sample CM-56 indicates carbonates with high Fe content (33%) and Mn (12%) content and low contents of Mg and Ca (<1%) for 12 analyses. Normalizing these data for carbonates shows a considerable amount of $MnCO_3$ (11–39.2 mole%) (Table 3). Spinels that occur as small undeformed grains (0.1–0.3 mm) generally show pitted dissolution textures (Figure 6a) with Fe (17.6%) and Mg (14%) as the principal components. The composition of magnetite crystals reaches 83.2% Fe.

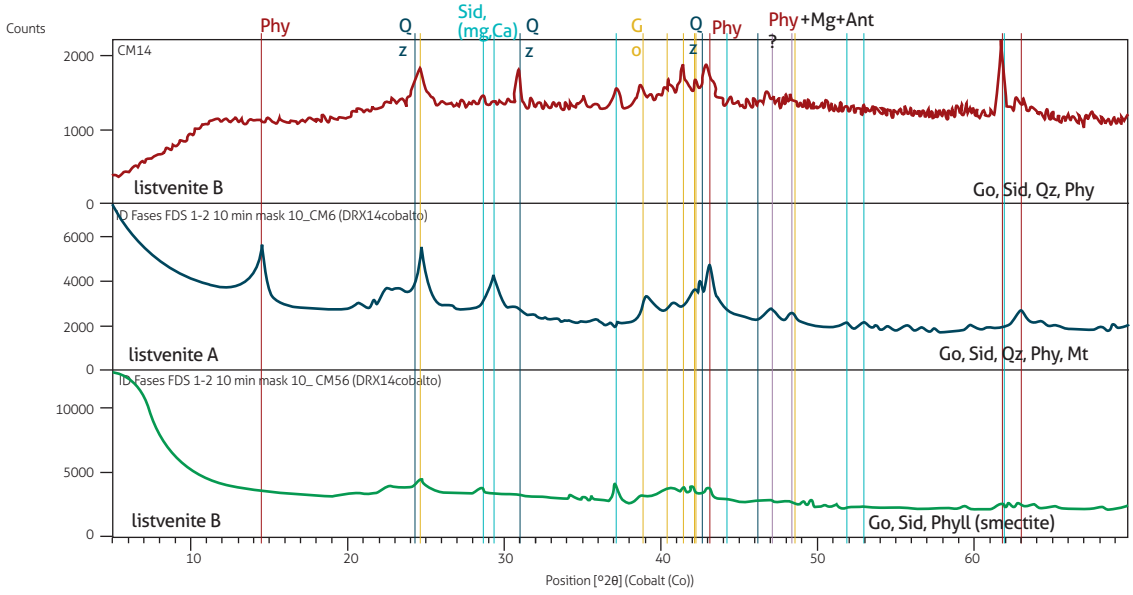

Figure 5. XRD diffractograms
XRD for fractions (>200 microns). Sample CM-3 contains the following: quartz (Qz), siderite (Sid), goethite (Go) and phyllosilicates (Phy). Sample CM-6 is composed of quartz, siderite, goethite, magnetite (Mt) and phyllosilicates. Sample CM-56 contains siderite, goethite and phyllosilicates.

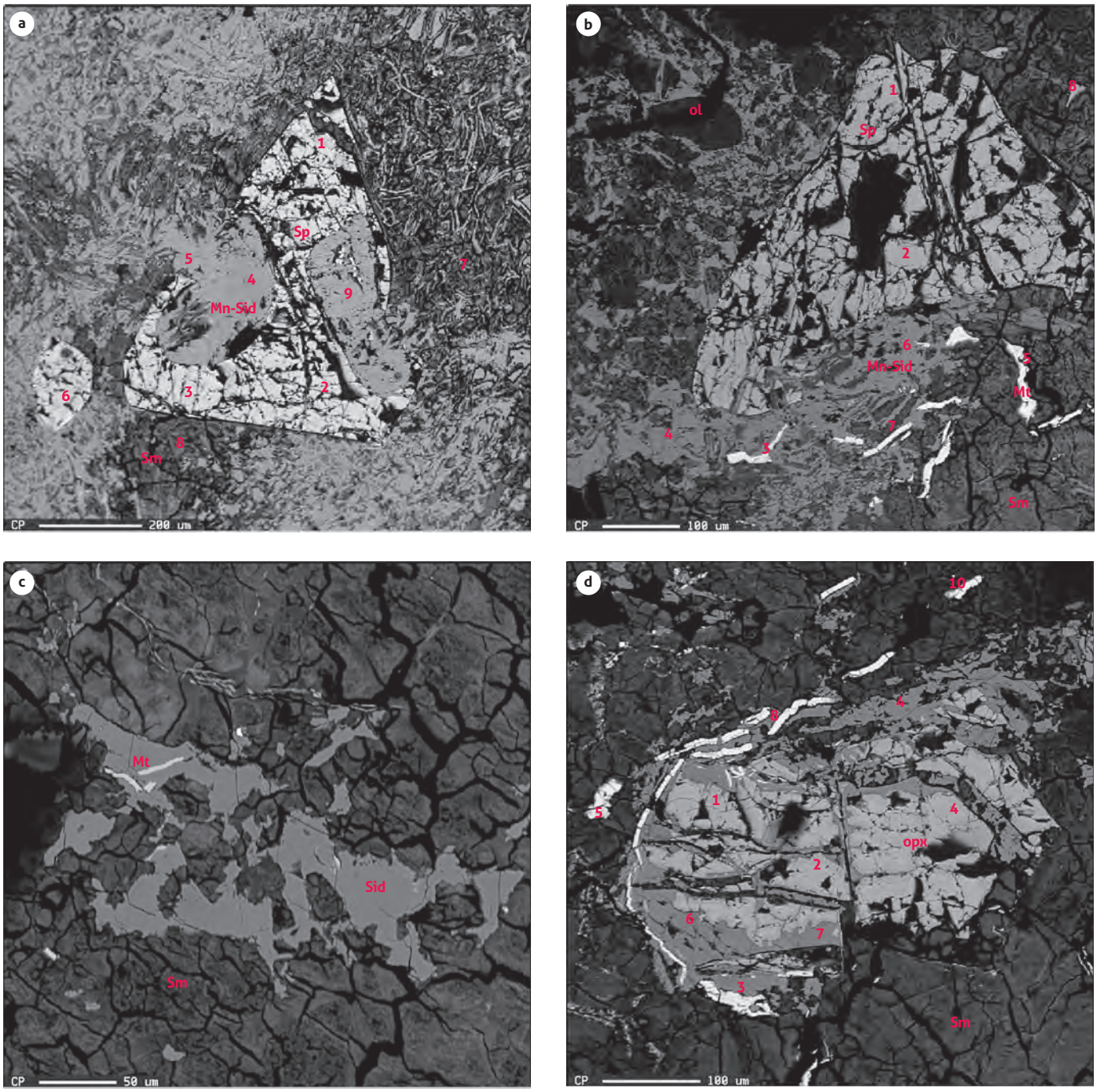

Figure 6. Scanning electron microscope analysis of the listvenite components in detail
a) Neoblastic texture of listvenite composed of smectite (Sm) and Mn-siderite (Mn-Sid) surrounding a euhedral Cr-spinel (Sp) fractured crystal that is partially altered. b) Smectite (Sm) and Mn-siderite (Mn-Sid) surrounded by Cr-spinel (Sp) euhedral crystals, magnetite (Mt), and olivine (Ol), which are accessories. c) Fractured smectite (Sm) with a substantial amount of siderite (Sid). d) Orthopyroxene (opx) altered to serpentine surrounded by smectite (Sm) and euhedral crystals of magnetite (Mt).

Table 2. Listvenites chemical composition in wt%

Name	wt (%)								MgO/SiO_2	Sample ID
	SiO_2	Al_2O_3	Fe_2O_3	MgO	CaO	MnO	TiO_2	Ni		
Listwaenite	27.54	4.2	61.8	2.3	0.2	0.8	0.05		0.086	CM-14
Tachylite	28	6.5	44.9	3.0	0.0	0.3	0.07	2.6	0.109	Gleeson et al. (2004)
Tachylite	37.1	3.8	25.2	17.4	0.2	0.1	<0.01	4.2	0.469	Gleeson et al. (2004)
Tachylite	53.1	2.9	22.9	3.7	0.1	1.6	<0.01	6.1	0.069	Gleeson et al. (2004)
Tachylite	65.3	2.7	21.5	1.8	<0.01	0.3	<0.01	1.6	0.027	Gleeson et al. (2004)
Peridotite	41.2	0.3	9	42.6	0.2	0.1	<0.01	0.2	1.033	Gleeson et al. (2004)
Peridotite	42	0.3	9	41.9	0.3	0.1	<0.01	0.2	0.997	Gleeson et al. (2004)
Peridotite	43.8	0.4	9.1	42.1	0.4	0.1	<0.01	0.2	0.962	Gleeson et al. (2004)
Tachylite A	42.8	3.4	28.4	4.1	0.5	0.4	N.D.	1.8	0.098	Sumicol (2002)
Tachylite B	39.5	2.2	34.3	1.0	0.3	1.3	N.D.	1.5	0.027	Sumicol (2002)

Comparation between listvenite (sample CM-56, XRF) and "tachylites" (ICP-AES) composition, data from Sumicol (2002) and Gleeson et al. (2004), both of which are given in wt%.

Table 3. Microprobe mean chemical composition of Mn-siderite in the Cerro Matoso listvenite sample CM-56.

Chemical composition of Mn-siderite in CM listvenites										
wt %	K_2O	Na_2O	MnO	SrO	CaO	MgO	FeO	BaO	CO_2	Total
Mean	0.01	0.09	12.44	0.01	0.16	0.97	33.00	0.01	29.18	75.86
Desv	0.01	0-04	3.90	0.01	0.06	0.28	6.82	0.02	1.77	4.77
mole %	K_2CO_3	Na_2CO_3	$MnCO_3$	$SrCO_3$	$CaCO_3$	$MgCO_3$	$FeCO_3$	$BaCO_3$	Total	
Mean	0.02	0.42	26.85	0.01	0.43	3.64	68.63	0.,01	100.00	
Desv	0.03	0.19	9.33	0.01	0.19	1.09	10.10	0.02	100.00	

Mn-siderite: 12 points analyzed

5. Discussion

The term listvenite has been used to principally describe the assemblage of carbonate + silica as the product of carbonation in mantle rocks (Buisson and Leblanc, 1987; Leblanc, 1991; Halls and Zhao, 1995; Nasir et al., 2007; Kelemen and Matter 2008; Bucher and Stober, 2019) but also in metamorphosed rocks (e.g., amphibole-bearing listvenites, Nosouhian et al., 2016). Listvenites can be classified based on their SiO_2 content as silica, silica-carbonate, and carbonate listvenites (e.g., Nasir et al., 2007; Aftabi and Zarrinkoub, 2013; Azer, 2013;) with mineralogical compositions similar to those described by Ucurum (2000) with the assemblage of quartz + calcite + dolomite + ankerite ± magnesite as major rock-forming minerals in silica-carbonate listvenites (Type I) and carbonate listvenite (Type II) composed of calcite + dolomite + ankerite with only trace amounts of quartz and magnesite; or with the assemblage of quartz + calcite + magnetite + goethite + hematite ± talc ± ankerite (e.g., listvenites in Turkey; Central Eastern Desert, Egypt; Tavreh mercury prospect, northwestern Iran; Sartohay ophiolitic mélange, Xinjiang, NW China; and Semail Ophiolite, Oman). At Cerro Matoso, on the contrary, listvenites are composed of siderite ± phyllosilicates and can either be accompanied by quartz or not accompanied by quartz. Commonly, the siderite is a Mn-siderite.

The Mn-carbonate in listvenites could be formed by replacing calcium carbonate with CO_2 derived from hydrothermal fluids, as suggested by Zierbeng and Shanks (1988). Furthermore, Mn enrichment has been associated with hydrothermal systems, hydrothermal deposits and hydrothermal sulfides (e.g., Von Damm, 1995; Dekov et al., 2004; Taitel-Goldman et al., 2008). Siderite and Mn-siderite crystallize better under reducing conditions of high CO_2 and partial pressure and at elevated dissolved iron or manganese concentrations. Nevertheless, additional chemical and geochemical analysis of the Mn-siderite at Cerro Matoso is necessary to confirm this formation mechanism.

The Mn-siderite in the type B listvenites (CM-56) conforms to a neoblastic texture with spinels and smectite instead of forming veins or filling fractures and is likely a product of

metasomatic alteration. Additionally, type A listvenites (CM-3, CM-4, CM-6, CM-7) with siderite and quartz forming vein systems indicate a pattern of fluid flow into the rocks.

Supported matrix breccia textures reflect the intensity of fracturing and hydrothermal vein fills and therefore the activity of fluids in the host rock. On the other hand, modified (QeM) and recrystallization textures (e.g., feathery texture) represent different hydrothermal phases or changes in the fluid conditions that allow morphological evolution of quartz, which, according to the presence of zoning textures, reflects abrupt changes in fluids and very advanced recrystallization processes.

In Cerro Matoso peridotites, weathering developed a complete laterite profile with complex silica vein stockwork at different topographic levels. It is commonly admitted that weathering of mantle peridotites tectonically exposed to the atmosphere commonly leads to natural carbonation processes through a mechanism that involves the infiltration of meteoric waters enriched in dissolved atmospheric CO_2. Mg and Si commonly released during the laterization of peridotites are usually represented by extensive cryptocrystalline silica/magnesite veins and widespread stockwork in the laterite profile, similar to the lowest area of Pit-1 in Cerro Matoso or in the New Caledonia ophiolites (Ulrich et al., 2014).

Based on field and textural observations at Bench level 42 and uppers, the carbonation of peridotites at Cerro Matoso must have gone through two stages to form the two types of listvenites that are associated with fracture zones, which act as pathways for altering and mineralizing fluids (e.g., Ucurum and Larson, 1999; Tsikouras et al., 2006). As suggested by Ucurum (2000), silica-carbonate listvenite is an early alteration product and is followed by non-quartz listvenites, which are formed as a final product from the alteration. The first stage produces a silica/carbonate vein system with brecciated textures affecting the type A listvenites at Cerro Matoso, and later the type B listvenites must have been formed. Listvenites of type A and B were apparently contemporaneous with the emplacement of the mantle section into the oceanic lithosphere, according to field relations. Abundant quartz veins (1 cm to 0.3 m wide) generated along fault zones with a regular pattern appear to have formed simultaneously with or slightly later than the listvenite. The most characteristic feature of listvenites is their relative resistance against weathering compared with the surrounding rocks.

The high silica content (65%) in the samples of listvenites (i.e., tachylites from Gleeson et al., 2004) compared with their possible precursors (peridotite, 45%) suggest an extra SiO_2 input in a metasomatic system. Additionally, it is associated with the intense quartz vein system pattern at the Cerro Matoso outcrops. Listvenites without quartz represent a second stage of metasomatic alteration. The latter are named carbonate listvenites (Type II) by Ucurum (2000), while those with quartz are named silica-carbonate listvenites (Type I) in the Karakuz area in Turkey. The lower content of SiO_2 in listvenite B (sample CM-3) (Table 2), although not identified by XRD, is part of the silica in phyllosilicates. This makes sense because silica is more soluble at higher pH levels, a setting that makes the formation of siderite favorable. This suggests that the hydrothermal solution to form the listvenites at Cerro Matoso was characterized by low to moderate temperatures under a reduced environment instead of an oxidized environment or supergene.

Although Barnes et al. (1973) suggest that in a supergene listvenitization, the amount of carbonate, silica, and the pH of the groundwaters favor the precipitation and recrystallization of carbonate and/or silica after or coincident with dissolution to create carbonated and/or silicified peridotites, Nasir et al. (2007) suggest that this process is more efficient with hydrothermal fluids at alkaline pHs. Stanger (1985) indicates that silicification of listvenites is a low-temperature chemical replacement feature and not a weathering phenomenon, although some effects leading to the formation of listvenite are aqueous precipitates from bicarbonate-rich groundwaters (Neal and Stanger, 1984, 1985; Stanger and Neal, 1984; Stanger, 1985).

However, the details about the petrogenesis of listvenites at Cerro Matoso are complicated and still not clearly defined, although fluids required for listvenitization will probably be related to low temperature hydrothermal systems of Type II (Kelley and Shank, 2010) in Castrillón (2019).

A low-temperature, alkaline, and highly reduced fluid, probably drained from serpentinite, could favor siderite formation instead of another carbonate. The low silica content (27-65%) compared with that of other listvenites (e.g., 85-92% in Koracakaya, Turkey; 81-83%, in the Iti ophiolite, Greece) also suggests that these rocks were affected by hydrothermal systems, increasing silica content in some cases (i.e., near veins) or reducing it in others. In the latter case, the possibility is that silica will dissolve from serpentinite and/or harzburgite into the hydrothermal fluid during the formation of type B listvenites and will be taken from the system by the remaining silica-rich fluid in a high-pH and low-temperature environment. This is

possible because silica is more soluble at high pH levels (>9) and could therefore indicate which listvenite is formed first.

Hydrothermal fluids apparently induced alteration of Cr-spinel to siderite. This fluid allowed an intense water-rock interaction resulting in carbonation, partial silicification, and less serpentinization of the peridotite (Nasir et al., 2007). The intensity of the alteration at the local level varies from small veins of carbonate and quartz to complex stockwork systems that replace the original structure of the rock. These vein structures can also be precipitated by weathering. To clarify this point, isotope analyses of siderite would be useful. Meanwhile, it is clear that listvenite lenses in Cerro Matoso can reach 20 m of thickness, can vary from a few meters to 200 m, and can vertically grade to the serpentinized harzburgites from which they were derived; these harzburgites had also suffered an intense supergene weathering process, which converted peridotites into green saprolites that also present siderite (Sumicol, 2002).

High Cr and Ni contents and the occurrence of Cr-spinel plus Mn-carbonate, olivine, and orthopyroxene relics indicate an ultramafic protolith for the Cerro Matoso listvenites. Ucurum (2000) indicates that elements such as As, Ba, Cr and Ni are more enriched in silicate-carbonate listvenites that were probably controlled by the amount and the presence of silica, which creates an increase in their concentration compared with the serpentinites' Co, Cr and Ni content. In this sense, Ni grades (reaching 6.1 wt%) of listvenites at Cerro Matoso could be associated with hydrothermal alteration of peridotites, as also happened for Co, Hg and Au, (Koc and Kadiglu, 1996) or for Ni, Mn, Pb, Co and SiO_2 (Aydal, 1990), rather than a supergene origin.

Differences in the amounts of Fe_2O_3, SiO_2 and MgO in the listvenites (A and B, Table 2) suggest differences in the alteration, intensity or composition of the protolith and/or the chemistry of the ancient hydrothermal fluids affecting the peridotites. High concentrations of Fe-Mn in the fluids should have favored the formation of siderite and Mn-siderite. Once exposed to supergene weathering conditions (since the Eocene), the chemistry of listvenites was possibly affected as well.

The difference of the presence of siderite instead of other carbonates in the Cerro Matoso listvenites may be because they are derived from fresh ultramafic rocks, such as those reported in Central Euboea, Greece (Capedri and Rossi, 1973). Listvenites generally comprise part of the hydrothermal transformation of ophiolitic melánges that contain a chaotic accumulation of harzburgite, lherzolite, dunite, chromitite, gabbro, diabase, basalt, tuff, and chert blocks (e.g., serpentinite bodies in the Divrigi and Kuluncan ophiolitic mélange, Turkey [Ucurum, 2000]; Sartohay ophiolitic mélange in west Junggar, Xinjiang, China [Qiu and Zhu, 2015, 2018]), which can contribute to the amount of carbonates it contains. The Egyptian ophiolites are described as variably dismembered, deformed, altered, and metamorphosed peridotites due to serpentinization and interaction with a large flux of CO_2-bearing fluids (Gahlan et al., 2018) that led to the formation of various types of carbonate-bearing meta-ultramafics, but also were tectonically incorporated in a mélange with metasediments and metavolcaniclastics (Gahlan et al., 2018). Siderite deposits are reported at the contact between Caltu ultramafic rock and the Buldudere Formation in the Kuluncak ophiolite mélange (Ucurum, 2000).

According to Kashahi and Allakverdiev (1965), listvenites are formed, with a few exceptions, by the metasomatic/hydrothermal alterations of serpentine to evolve as products in two successive stages of the same process: the serpentinization of ultrabasites followed by metasomatic alteration. Similarly, Ucurum (2000) shows that listvenite is formed later than serpentinization and is superimposed on earlier serpentinite, which means that lisvenitization occurs by metasomatism of weakly serpentinized or completely serpentinized mafic minerals.

A fossilized Type II hydrothermal system (Kelly and Shank, 2010) was proposed as part of the geological history of Cerro Matoso (Castrillón, 2019) based on the isotope composition in bulk samples in black conglomeratic mudstone (BCM) overlying listvenites. Although negative $\delta^{13}C$ (-21.6 to -8.1‰ V-PDB) values are compatible with meteoric waters, $\delta^{18}O$ (25.1 to 29.8 ‰ V-SMOW) values indicate a low-temperature hydrothermal/diagenetic system and could only be explained by oxidation of methane processes. It is possible that hydrothermal fluid activity metasomatized the Cerro Matoso peridotites. According to information from a hole drilled at Pit-1 (Figure 1), listvenites have always been associated with BCM; unfortunately, some rocks with a similar chemical composition to listvenites were assigned the same name (i.e., tachylites by the mine geologists), and later, they were identified as marine sediments, generating confusion about the origin of both.

The $\delta^{18}O$ values at Cerro Matoso differ from the isotopic composition values of typical smectites of weathered clays (Savin and Epstein, 1970), which are consistent with $\delta^{18}O$ values (20.3 to 24.3 ‰ SMOW) in nickel smectites in Murrin Murrin, Western Australia (Gaudin et al., 2005), and represent water-rock interactions at low temperatures by the contact of

meteoric fluid during mineral leaching processes in which laterites are formed. These $\delta^{18}O$ isotope values in siderite form the BCM II facies, and some intraclasts indicate temperatures over 90°C that can be associated with diagenetic/hydrothermal fluids. These values are similar in temperature to the calculation from the $\delta^{18}O$ content of carbonate of silica-carbonate alteration (between 56°C and 163°C) of the Cretaceous ophiolite at Narman (Ucurum, 2000).

Most likely, as suggested (Kim et al., 2007), the slight difference of 0.00042 at 75°C in the fractionation factor between aragonite (Δ = 1.00856) and siderite (Δ = 1.00898) permitted the siderite to replace the original carbonate, inheriting its isotopic composition; however, according to Rosenbaum and Sheppard (1986), the minimal difference of 0.0002 at 100°C in the fractionation factor between ankerite (Δ = 1.00901) and siderite (Δ = 1.00881) could make it possible that siderite replaces ankerite, inheriting its isotopic composition. This would explain the presence of siderite instead of another carbonate in listvenites. Zheng (1998) also suggests that carbonates may prefer to be formed in the first state of crystallization of $CaCO_3$ and subsequently converted to another carbonate without isotopic reset.

Some ultramafic bodies in western Colombia have been associated with Pacific oceanic crust (Pindell and Barrett, 1990; Pindell and Kennan, 2009), as is the case for Cerro Matoso peridotites, where listvenites could have been formed in the oceanic domain in a pre- or syn-obduction context similar to the one suggested by Kishida and Kerrich (1987), Buisson and Leblanc (1987), Auclair et al. (1993) or Tsikouras et al. (2006), and would be the unusual expression of metasomatism in the ocean floor. Nevertheless, Nasir et al. (2007) suggest that the metasomatism process can take place either while an ophiolite is part of the oceanic lithosphere or during its detachment from it and be reflected along major thrust and fracture zones where the metasomatic alteration of the peridotite is more intense and complete.

Specifically, in an oceanic geological setting where the ophiolites are exposed at the seafloor, the peridotites undergo serpentinization reactions, and it is very possible that Type II hydrothermal systems (Kelley and Shanks, 2010) have been hosted in peridotites (e.g., Logatchev and Rainbow at the Mid-Atlantic Ridge). The additional geological setting, including the hydrothermal system hosted by the Cerro Matoso peridotites, in an ancient mid-oceanic ridge far west of its present location could have originated the metasomatic alteration of peridotites, and listvenites would be proof of that. After being accreted during the Cretaceous to the continent and strongly affected by weathering and mineral leaching processes since the late Eocene (López-Rendón, 1986), all of the rocks at Cerro Matoso changed chemically and physically, probably confusing the origins of some of them (i.e., black conglomeratic mudstone and listvenites).

6. Conclusions

The previously described unit has been defined since the end of the 20th century by geologists at Cerro Matoso S.A. (today, South32) as "tachylite", and it has been mineralogically and chemically described in studies by Sumicol (2002) and Gleeson et al. (2004), among others. Now, the term "listvenite" is assigned to this unit, meaning, in a broad sense, a product of siliceous-carbonated alteration of serpentinized ultramafic protolith by hydrothermal fluids.

The listvenite bodies at Cerro Matoso present a WNW-ESE orientation can be associated with fault zones through which hydrothermal fluids could have affected the original protolith (i.e., variably serpentinized harzburgite), altering the peridotite composition to produce an assemblage of Mn-siderite (12 wt%, MnO) +/- quartz, accompanied by nontronite, serpentine (lizardite ± chrysotile), goethite, and magnetite, with Cr-spinel relicts, olivine and orthopyroxene.

Field relations and textural evidence along with the occurrence of Cr-spinel relics suggest a hydrothermal metasomatism process that occurred before the supergene weathering of peridotite (of harzburgitic origin), perhaps during serpentinization processes once the Cerro Matoso peridotites were exposed in the ocean deep.

Acknowledgments

This article is part of the doctoral thesis of Andrés Castrillón, who gives thanks for a grant from Colciencias (Scholarship 647, National Doctorate) and Universidad Nacional de Colombia. This work was also possible thanks to the support of Dr. Vanessa Cole from the Universidad Nacional Autónoma de México and their team at the Instituto de Geología. Special acknowledgments go to the Cerro Matoso S.A. company for allowing the development of this research.

References

Abuamarah, B. A. (2020). Geochemistry and fore-arc evolution of upper mantle peridotites in the Cryogenian Bir Umq ophiolite, Arabian Shield, Saudi Arabia. *International Geology Review*, *62*(5), 630-648. https://doi.org/10.1080/00206814.2019.1652942

Aftabi, A., & Zarrinkoub, M. H. (2013). Petrogeochemistry of listvenite association in metaophiolites of Sahlabad region, eastern Iran: Implications for possible epigenetic Cu–Au ore exploration in metaophiolites. *Lithos*, *156-159*, 186-203. https://doi.org/10.1016/j.lithos.2012.11.006

Ash, C. H., & Arksey, R. L. (1991). *The listwaenites-lode gold association in British Columbia. Geological Fieldwork 1989*, paper 1990-1991.

Ash, C. H. (2001). *Relationship between ophiolites and gold–quartz veins in the North American Cordillera*. Bulletin 108. British Columbia, Ministry of Energy and Mines.

Auclair, M., Gauthier, M., Trottier, J., Jébrak, M., & Chartrand, F. (1993). Mineralogy, geochemistry, and paragenesis of the Eastern Metals serpentinite-associated Ni–Cu–Zn deposit, Quebec Appalachians. *Economic Geology*, *88*(1), 123-138. https://doi.org/10.2113/gsecongeo.88.1.123

Aydal, D. (1989). Gold-bearing listwanites in Arac Massif, Kastamonu, Turkey. *Terra Nova*, *2*(1), 43-52. https://doi.org/10.1111/j.1365-3121.1990.tb00035.x

Azer, M. K. (2013). Evolution and economic significance of listwaenites associated with Neoproterozoic ophiolites in South Eastern Desert, Egypt. *Geologica Acta*, *11*(1), 113-128. https://doi.org/10.1344/105.000001777

Barnes, I., O'Neil, J. R., Rapp, J. B., & White, D. E. (1973). Silica-carbonate alteration of serpentine: wall rock alterations in mercury deposits of the California Coast Ranges. *Economic Geology*, *68*(3), 388-398. https://doi.org/10.2113/gsecongeo.68.3.388

Barrero, D. (1974). *Metamorfismo regional en el Occidente Colombiano*. Simposio sobre ofiolitas Medellín, Colombia, Medellín.

Bates, R., & Jackson, J. (1987). *Glossary of Geology* (Third Ed.). American Geological Institute.

Boskabadi, A., Pitcairn, I. K., Broman, C., Boyce, A., Teagle, D. A. H., Cooper, M. J., Azer, M. K., Mohamed, F. H., Stern, R. J., & Majka, J. (2017). Carbonate alteration of ophiolitic rocks in the Arabian–Nubian Shield of Egypt: sources and compositions of the carbonating fluid and implications for the formation of Au deposits. *International Geology Review*, *59*(4), 391-419. https://doi.org/10.1080/00206814.2016.1227281

Bucher, K., & Stober, I. (2019). Interaction of Mantle Rocks with Crustal Fluids: Sagvandites of the Scandinavian Caledonides. *Journal of Earth Science*, *30*, 1084-1094. https://doi.org/10.1007/s12583-019-1257-2

Buisson, G., & Leblanc, M. (1987). Gold in mantle peridotites from Upper Proterozoic ophiolites in Arabia, Mali, and Morocco. *Economic Geology*, *82*(8), 2092-2097. https://doi.org/10.2113/gsecongeo.82.8.2091

Capedri, S., & Rossi, A. (1973). Conditions governing the formation of ophicalcites and listwaenites (Central Euboea/Greece). *Bulletin of Geological Society of Greece*, *10*(2), pp. 78-297.

Castrillón, A. (2013). *Determinación de las estructuras tubulares presentes en el Pit 6 en el depósito laterítico de níquel de Cerro Matoso* (Master thesis). Universidad Nacional de Colombia.

Castrillón, A. (2019). *Carbonatos y otros minerales autigénicos asociados a las lateritas niquelíferas de Cerro Matoso y su posible relación con actividad hidrotermal y reducción de sulfatos* (Doctoral Thesis) Universidad Nacional de Colombia.

Dekov, V. M., & Savelli, C. (2004). Hydrothermal activity in the SE Tyrrhenian Sea: an overview of 30 years of research. *Marine Geology*, *204*(1-2), 161-185. https://doi.org/10.1016/S0025-3227(03)00355-4

Demoustier, A. (1995). *Contribution ala caractérisation des quartz auriferes de la région de Cabo de Gata, province d'Almería, Espagne. Pétrographie-thermoluminescence-inclu-sions fluides. Travail de fin d'études*, Faculté Polytechnique de Mons.

Demoustier, A., & Castroviejo, R. (1997). *Fluid inclusion characterization of the Carneros epithermal ores (Cabo de Gata, Almería, SE Spain): preliminary results*. XIV ECROFI (European Current Research on Fluid Inclusions), Nancy, France.

Demoustier, A., Castroviejo, R., & Charlett, J. M. (1998). Clasificación textural del cuarzo epitermal (Au-Ag) de relleno filoniano del area volcánica de Cabo de Gata, Almeria. *Boletín Geológico y Minero*, *109*(5-6), 449-468.

Gahlan, H. A., Azer, M. K., & Asimow, P. D. (2018). On the relative timing of listwaenite formation and chromian spinel equilibration in serpentinites. *American Mineralogist*, *103*(7), 1087-1102. https://doi.org/10.2138/am-2018-6473

Gaudin, A., Decarreau, A., Noack, Y., & Grauby, O. (2005). Clay mineralogy of the nickel laterite ore developed from serpentinised peridotites at Murrin Murrin, Western Australia. *Australian Journal of Earth Sciences*, *52*(2), 231-241. https://doi.org/10.1080/08120090500139406

Gleeson, S., Herrington, R., Durango, J., & Velazquez, C. (2004). The Mineralogy and Geochemistry of the Cerro Matoso S.A. Ni Laterite Deposit, Montelíbano, Córdoba. *Economic Geology, 99*(6), 1197-1213. https://doi.org/10.2113/gsecongeo.99.6.1197

Gonçalves, C., Fabris, J., & Pacheco Serrano, W. (1999). Chemical and mineralogical analyses of a weathering mantle developing on peridotite of the mining area for nickel in Cerro Matoso, Colombia. *Hyperfine Interactions*, 122, 171-176. https://doi.org/10.1023/A:1012658009195

Halls, C., & Zhao, R. (1995). Listvenite and related rocks: perspectives on terminology and mineralogy with reference to an occurrence at Cregganbaun, Co. Mayo, Republic of Ireland. *Mineralium Deposita*, *30*(3-4), 303-313. https://doi.org/10.1007/BF00196366

Imamalipour, A., Karimlou, M., & Hajalilo, B. (2018). Geochemical zonality coefficients in the primary halo of Tavreh mercury prospect, northwestern Iran: implications for exploration of listwaenitic type mercury deposits. *Geochemistry: Exploration, Environment, Analysis*, *19*(4), 347-357. https://doi.org/10.1144/geochem2018-048

Jutras, J., & Geol, P. (2002). Ultramafic nickel-bearing magmas of the Nadaleen river area (106C/3) and associated listwaenites: new exploration targets in Mayo Mining District, Yukon. In D. Emond, & L. Lewis, *Exploration and Geological Service Division, Yukon Region, Indian and Northerb Affairs, Canada*. Manson Creek Resources Ltda.

Kashkai, M., & Allakverdiev, S. (1965). *Listwaenites, their origin and classification.* (U. G. Survey, Ed.) Baku, Izdat. Akad, Nauk Azerbaidzhanskoi: Translated by Vi-taliano, D.B.

Kelemen, P. B., & Matter, J. M. (2008). In situ carbonation of peridotite for CO_2 storage. *PNAS*, *105*(45), 17295-17300. https://doi.org/10.1073/pnas.0805794105

Kelley, D. S., & Shank, T. M. (2010). Hydrothermal systems: a decade of discovery in slow spreading environments. In P.a. Rona, C.w. Devey, J. Dyment, & B.j. Murton (Eds.), *Diversity Of Hydrothermal Systems On Slow-Spreading Ocean Ridges*. Agu Geophysical Monograph Series. https://Doi.org/10.1029/2010Gm000945

Kim, S-T., Mucci, A., & Taylor, B. E. (2007). Phosphoric acid fractionation factors for calcite and aragonite between 25 and 75 °C: Revisited. *Chemical Geology*, *246*(3-4), 135-146. https://doi.org/10.1016/j.chemgeo.2007.08.005

Kishida, A., & Kerrich, R. (1987). Hydrothermal alteration zoning and gold concentration at the Kerr–Addison Archean lode gold deposit, Kirkland Lake, Ontario. *Economic Geology*, *82*(3), 649-690. https://doi.org/10.2113/gsecongeo.82.3.649

Koc, S., & Kadioglu, Y. K. (1996). Mineralogy, geochemistry, and precious metal content of Karacakaya (Yunusemre-Eskisehir) Listwaenites. *Ofioliti*, *21*(2), 125-130.

Leblanc, M. (1991). Platinum-group elements and gold in ophiolitic complexes: distribution and fractionation from mantle to oceanic floor. In T. Peters, A. Nicolas, & R. Coleman, *Ophiolite Genesis and Evolution of the Oceanic Lithosphere*. Springer. https://doi.org/10.1007/978-94-011-3358-6_13

Lelis, M.deF., Gonçalvesa C. M., Fabris, J. D., Mussel, W. N., & Pacheco-Serrano, W. A. (2004). Effectiveness of Selective Chemical Treatments on Concentrating Magnetic Minerals of Samples from a Nickel-Ore Peridotite Mantle. *Journal of the Brazilian Chemical Society*, *15*(6), 884-889. https://doi.org/10.1590/S0103-50532004000600015

Lewis, J., Draper, G., Proenza, J., Epaillat, J., & Jiménez, J. (2006). Ophiolite-Related Ultramafic Rocks (Serpentinites) in the Caribbean Region: A Review of their ocurrence, composition, origin, emplacement and Ni-laterite soil formation. *Geológica Acta, 4*(1-2), 237-263. https://doi.org/10.1344/105.000000368

Londoño, A. C., & González, H. (1997). *Geología del Departamento de Córdoba*, Scale 1:250.000. Ingeominas.

López-Rendón, J. (1986). *Geology, Mineralogy and Geochemistry of the Cerro Matoso Nicheliferous Laterite, Córdoba, Colombia.* Montelibano (Master Thesis). Colorado State University.

Meissner, R., Flueh, E., Stibane, F., & Berg, E. (1976). Dynamics of the active plate boundary in soutwest Colombia according to recent geophysical measurements. *Tectonophysics*, *35*(1-3), 115-136. https://doi.org/10.1016/0040-1951(76)90032-9

Mejia, V., & Durango, J. (1981). Geologia de las lateritas niquelíferas de Cerro Matoso. *Boletin de Geología, 15*(29), 117-123.

Mora-Bohórquez, J., Ibáñez-Mejía, M., Oncken, O., de Freitas, M., Vélez, V., Mesa, A., & Serna, L. (2017). Structure and age of the Lower Magdalena Valley basin basement, northern Colombia: New reflection-seismic and U-Pb-Hf insights into the termination of the central andes against the Caribbean basin. *Journal of South American Earth Sciences*, 74, 1-26. https://doi.org/10.1016/j.jsames.2017.01.001

Nasir, S., Al Sayigh, A., Al Harthy, A., Al-Khirbash, S., Al-Jaaidi, O., Musllam, A., Al-Mishwat, A., & Al-Bu'saidi, S. (2007). Mineralogical and geochimical characterization of listwaenite from the Semail Ophiolite, Oman. *Geochemistry*, *67*(3), 213-228. https://doi.org/10.1016/j.chemer.2005.01.003

Neal, C., & Stanger, G. (1983). Hydrogen generation from mantle source rocks in Oman. *Earth and Planetary Science Letters*, *66*, 315-320. https://doi.org/10.1016/0012-821X(83)90144-9

Neal, C., & Stanger, G. (1984). Calcium and magnesium hydroxide precipitation from alkaline groundwaters in Oman, and their significance to the process of serpentinization. *Mineralogical Magazine*, *48*(37), 237-241. https://doi.org/10.1180/minmag.1984.048.347.07

Neal, C., & Stanger, G. (1985). Past and present serpentinization of ultramafic rocks; an example from the Semail ophiolite nappe of northern Oman. In J.I. Drever (ed.), *The Chemistry of Weathering. Reidel*, Dordrecht

Nosouhian, N., Torabi, G., & Arai, S. (2016). Amphibole-bearing listwaenites from the Paleozoic Bayazeh ophiolite (Central Iran). *Italian Journal of Geosciences*, *135*(1), 109-119. https://doi.org/10.3301/IJG.2015.04

Nosohuian, N., Torabi, G., & Arai, S. (2019). Petrological aspects of the Bayazeh Paleozoic ophiolite (Central Iran); implications for Paleo-Tethys subduction. *Periodico di Mineralogia*, *88*(2), 155-184.

Pindell, J., & Barrett, S. (1990). Geological evolution of the Caribbean region: a plate tectonic perspective. In J. Pindell, & S. Barrett, *The Caribbean Decade of North American Geology*. Geological Society of America.

Pindell, J., & Kennan, L. (2009). Tectonic evolution of the Caribbean and northern South America in the mante reference frame. In J. Pindell, & L. Kennan, *The geology and evolution of theh region between North and South America* (Special Publication ed., p. 60). Geological Society of London.

Qiu, T., & Zhu, Y. F. (2015). Geology and geochemistry of listwaenite-related gold mineralization in the Sayi gold deposit, Xinjiang, NW China. *Ore Geology Reviews*, *70*, 61-79. https://doi.org/10.1016/j.oregeorev.2015.03.017

Qiu, T., & Zhu, Y. F. (2018). Chromian spinels in highly altered ultramafic rocks from the Sartohay ophiolitic mélange, Xinjiang, NW China. *Journal of Asian Earth Sciences*, *159*, 155-184. https://doi.org/10.1016/j.jseaes.2017.08.011

Rose, G. (1837). Mineralogisch-geognostiche Reise nach dem Ural, dem Altai und dem Kaspischen Meere. In C. Berlin, *Eichoff (Verlag der Sanderchen Buchhandl)* (Vols. I-VII).

Rosenbaum, J., & Sheppard, S. (1986). An isotopic study of siderites, dolomites and ankerites at high temperatures. *Geochimica et Cosmochimica Acta*, *50*(6), 1147-1150. https://doi.org/10.1016/0016-7037(86)90396-0

Savin, S. M., & Epstein, S. (1970). The oxygen and hydrogen isotope geochemistry of clay minerals. Geochimica et Cosmochimica Acta, *34*(1), 25-42. https://doi.org/10.1016/0016-7037(70)90149-3

Stanger, G., & Neal, C. (1984). A new occurrence of suoluinte, from Oman. *Mineralogical Magazine*, *48*, 143-146.

Stanger, G. (1985). Silicified serpentinite in the Semail nappe of Oman. *Lithos*, *18*, 13-22. https://doi.org/10.1016/0024-4937(85)90003-9

Sumicol S.A. (2002). *Caracterización mineralógica de los tipos de roca de la laterita niquelífera de Cerro Matoso S.A., Colombia*. Informe privado para Cerro Matoso S.A., 2 vols.

Taitel-Goldman, N., Ezersky, V., & Mogilyanski, D. (2008). Study of Mn-siderite–rhodochrosite from the hydrothermal sediments of the Atlantis II Deep, Red Sea. *Israel Journal of Earth Sciences*, *57*, 45-54.

Tsikouras, B., Karipi, S, Grammatikopoulos, T. A., & Hatzipanagiotou, K. (2006). Listwaenite evolution in the ophiolite mélange of Iti Mountain (continental Central Greece). *European Journal of Mineralogy*, *18*(2), 243-255. https://doi.org/10.1127/0935-1221/2006/0018-0243

Ucurum, A. (1998). Application of the correspondence-type geoestatistical analysis on the Co, Ni, As, Ag, and Au concentrations of the listwaenites from serpentinites in the Diveru and Kulunack ophiolitic mélanges. *Turkish Journal of Earth Sciences*, *7*(2), 87-95.

Ucurum, A., & Larson, L. T. (1999). Geology, Base-Precious Metal Concentration and Genesis of the Silica-Carbonate Alteration (Listwaenites) From Late Cretaceous Ophiolitic Mélanges at Central East Turkey. *Chemie der Erde*, 59, 77-104.

Ucurum, A. (2000). Listwaenites in Turkey: perspectives on formation and precious metal concentration with referene to occurrences in East-Central Anatolia. *Ofioliti*, *25*(1), 15-29.

Ulrich, M., Muñoz, M., Guillot, S., Cathelineau, M., Picard, C., Quesnel, B., Boulvais, P., & Couteau, C. (2014). Dissolution–precipitation processes governing the carbonation and silicification of the serpentinite sole of the New Caledonia ophiolite. *Contributions to Mineralogy and Petrology*, *167*. https://doi.org/10.1007/s00410-013-0952-8

Von Damm, K. L. (1995). Controls on the chemistry and temporal variability of seafloor hydrothermal fluids. In S. Humphris, J. Lupton, L. Mullineaux, & R. Zierenberg, (eds.), *Physical, Chemical, Biological, and Geological Interactions within Seafloor Hydrothermal Systems*, vol. 91, 222-247. https://doi.org/10.1029/GM091p0222

Zheng, Y. F., Fu, B., Li, Y., Xiao, Y., & Li, S. (1998). Oxygen and hydrogen isotope geochemistry of ultra-high pressure eclogites from the Dabie mountains and the Sulu terrane. *Earth and Planetary Science Letters*, *155*(1-2), 113-129. https://doi.org/10.1016/S0012-821X(97)00203-3

Zierenberg, R. A., & Shanks, W. C. (1988). Isotopic studies on epi- genetic features in metalliferous sediment Atlantis II Deep, Red Sea. The Canadian Mineralogist, 26(3), 737-753.